



OPEN

Synergistic effects of titanium dioxide and graphene nanofillers on delamination and thrust forces in machining glass fiber reinforced nanocomposites

Machabhaktuni Sri Harsha¹, Vennelakanti Sai Hemanth Kumar¹, Mandapati Bhavani Prasad¹, Chandrasekar Muthukumar¹, Senthil Muthu Kumar Thiagamani^{2,3,4}, Nadir Ayrilmis⁵, Senthilkumar Krishnasamy⁶, Lin Feng Ng^{4,7} & Naveen Jesuarockiam⁸

Delamination factor in drilling represents the maximum spread of imperfections around the drilled hole in a polymer composite. D_f can directly affect the performance of the drilled component. This study focuses on investigating the influence of nanofillers, titanium dioxide and graphene, with epoxy in varying quantities ranging from 1 to 4 wt%, on the delamination behavior of the glass fiber-reinforced composites. The parameters, such as spindle speeds (600, 1200, and 1800 rpm), feed rates (30, 40, and 50 mm/min), and drill bit diameter (4, 6, and 8 mm), were considered. A high-resolution camera was used to capture the images of the drilled hole, which were processed using MATLAB to compute the delamination factor at top and rear faces of the composite. Additionally, thrust force obtained from the dynamometer at various nanofiller quantities was analyzed. The thrust force decreased with an increase in the spindle speed and the feed rate. Spindle speed and feed rate contributed the least to delamination, while filler percentage contributed the least to thrust. The mean GRG showed that GT1, a drill bit diameter of 4 mm, a spindle speed of 1800 rpm and a feed rate of 50 mm/min were the optimum parameters.

Keywords Polymer composites, Nanofillers, Drilling performance, Delamination

Due to their unique mechanical properties, composite materials are in high demand in all engineering applications. However, there is a growing need for materials with superior properties for better operational performance. A proven way of enhancing the performance of composites is by dispersing the matrix phase with a small quantity of nanoparticles. When such materials are to be replaced with conventional composites, it is inevitable to understand their behavior under various mechanical loads as well as to select optimum parameters under different drilling and machining methods¹.

To fabricate components in any industry, the glass fiber-reinforced composites (GFRPC) undergo specific operations such as grinding, milling, and drilling, especially for fastening purposes. Among the mentioned operations, drilling is widely used as the most suitable operation for creating holes in composite materials. For instance, a small aircraft engine requires a minimum of 100,000 holes². However, it is crucial to consider some potential damage that could occur during the drilling operations. For instance, fiber pull-out, fiber breakage, matrix cracking, and matrix-fiber debonding. These damages significantly influence the mechanical strength of

¹SIMCRASH Centre, Department of Aerospace Engineering, Hindustan Institute of Technology and Science, Kelambakkam, Chennai 603103, India. ²Department of Mechanical Engineering, Kalasalingam Academy of Research and Education, Anand Nagar, Krishnankoil 626126, Tamil Nadu, India. ³Department of Mechanical Engineering, INTI International University, Persiaran Perdana BBN, Putra Nilai, Nilai 71800, Negeri Sembilan, Malaysia. ⁴Centre for Advanced Composite Materials (CACM), Universiti Teknologi Malaysia, Skudai, Johor Bahru 81310, Johor, Malaysia. ⁵Department of Wood Mechanics and Technology, Faculty of Forestry, Istanbul University-Cerrahpasa, Bahcekoy, Sarıyer 34473, Istanbul, Turkey. ⁶Department of Mechanical Engineering, PSG Institute of Technology and Applied Research, Coimbatore, Tamil Nadu, India. ⁷Faculty of Mechanical Engineering, Universiti Teknologi Malaysia, Skudai, Johor Bahru 81310, Johor, Malaysia. ⁸School of Mechanical Engineering, Vellore Institute of Technology, Vellore 632014, Tamil Nadu, India. email: tsmkumar@klu.ac.in; nadiray@iuc.edu.tr

the fabricated components. Common damage in drilling holes is delamination. Two delamination terminologies known as peel-up delamination at the top face and push-out delamination at the rear face of the composite relate to the maximum area covered due to the imperfections around the drilled hole. Due to delamination assembly tolerances decrease resulting in declining material performance over time. In aircrafts 60% of manufactured parts are rejected due to damage caused by delamination^{3,4}. The financial implications of drilling-induced delamination have motivated researchers to continuously minimize such damage.

Drilling experiments on the GFRPC have been extensively studied and have been well documented in the literature. In their work, Mohan et al.⁵, revealed that the cutting speed influenced peel-up delamination, whereas feed rate influenced the push-down delamination. In another study, Ghasemi et al.⁶, indicated that extreme feed rate values, drill rotation speed, and drill point angle contributed to higher delamination in the GFRPC laminates. In summary, these findings emphasize the importance of selecting suitable drilling parameters to minimize delamination and, at the same time, indicate the existence of optimum parameters in multiple input characteristics of the GFRPC. Various techniques like particle swarm optimization (PSO), response surface methodology (RSM), artificial neural networks, Taguchi's orthogonal array, Grey relational analysis, and genetic algorithms have been utilized by researchers to obtain the optimum combination of the process parameters for single and multi-response input characteristics⁷.

In order to enhance the mechanical properties of composites, the introduction of nanoparticles into composite materials has gained significant interest in the field. The addition of multi-walled carbon nanotubes to the GFRP improved the CAI (Compression After Impact) and charpy impact properties of the specimens in the thermoset composites⁸. Improvements in thermal stability, flexural strength, and dielectric properties in polyimide/glass Fibre (PI/GF) hybrid material with polyhedral oligomeric silsesquioxanes (POSSs) and silica nanofillers were shown, concluding that inorganic fillers could also be viable nanofillers depending on desired mechanical properties⁹. In a previous study¹⁰, it was reported that titanium dioxide-infused glass-reinforced fiber epoxy composites showed a 37% increase in flexural strength and a 28% increase in flexural modulus compared to normal glass-reinforced fiber epoxy composites. Other works by Singh et al.¹¹ and Abass et al.¹² also showed a positive correlation in the increase of flexural properties in titanium dioxide (TiO_2)-infused glass-reinforced fiber epoxy composite. In the work of Tüzemen et al.¹³, nanographene glass-reinforced fiber epoxy composites showed an increase in tensile strength, deformation, modulus of elasticity, and toughness. Significant improvements in the tensile strength of 32.8% with the addition of 0.25 wt% of TiO_2 , and enhancement of the tensile modulus of 74.5% with the addition of 0.5 wt% of TiO_2 were also observed¹⁴. This concludes that titanium dioxide and graphene have positive effects on the mechanical properties of the GFRC. El-Ghaoui, Khalid et al.¹⁵ worked on drilling unidirectional GFRP with graphene concluded that the addition of graphene resulted in an increase in thermal conductivity, thereby lowering the cutting temperature, causing thermal damage to the epoxy, and improving the machinability of the composite. Kumar et al.¹⁶ studied influence of graphene wt% on machining nanocomposites, suggesting addition of graphene reduces cutting force at high speeds but had positive effects only at the initial stage of thrust force. Thakur et al.¹⁷ conducted a review on effect of different fillers in machining composites and concluded fillers in matrix might improve or decline the performance of composite after machining. Kharwar et al.¹⁸ performed machining on multiwall carbon nanotubes reinforced epoxy composites and concluded that surface damages were reduced during machining due to improvement in thermal conductivity.

Due to superior properties of graphene and titanium dioxide many studies have been conducted on evaluating mechanical properties of GFRP dispersed either with titanium dioxide or with graphene nanofillers. Enhancing the machinability of composites with different tool geometries, different drilling parameters have also been investigated in the past decade. Limited studies investigated the influence of nanofillers (mostly carbon based) on machining performance of composites. However, there are no studies characterizing the machining behavior of GFRP combining with both titanium dioxide and graphene nanofillers. In this study, the influence of combining titanium dioxide and graphene nanofillers and its wt% on drilling performance of GFRP composites at various drilling conditions such as drill bit diameter, spindle speed, feed rate was investigated to determine the optimum drilling conditions.

Experimental procedure

Materials

Epoxy resin and hardener of matrix material were procured from Vasavibala Resins Pvt. Limited, Chennai. Fiberglass was supplied by M/s. Go Green Products, Chennai, India. Nano titanium dioxide (TiO_2) and nano graphene were procured from Ganapathi Scientific Co., Sriliviputhur, India. The constituent properties of the materials used in this research are shown in Table 1.

Fabrication of nanocomposites

Glass fiber composites with equal proportions of titanium dioxide and graphene nanofillers contributing to a total wt% of 1%, 2%, 3% and 4% were fabricated. Generally, by adding a lower percentage of nanofillers < 3% wt. increase mechanical properties of composites such as tensile strength by 60%^{19,20} and adding high wt% of nanofillers will deteriorate the mechanical properties of composites¹⁵. As a result, 1–4% wt% of nanofillers were considered in this study. Fabrication of a 1 wt% GFRP nanocomposite is described here. Graphene of 0.5% wt. and titanium dioxide of 0.5% wt. resulting in a total wt% of 1% were dispersed into the resin gradually using a mechanical stirrer operated at 500 rpm for 30 min. Then the hardener was added to this mixture in the ratio of 10:1 and mixed thoroughly. The fiberglass fabric is cut into 300×300 mm² sheets and impregnated with the resin mixture using a brush to ensure complete wetting of the fiberglass fabric. Five layers of those impregnated fiberglass fabric sheets are placed in a mold of size $300 \times 300 \times 4$ mm³ and the resin mixture is poured upon it.

| Matrix and reinforcement materials | Fiber glass | LY556 epoxy resin | HY951 epoxy hardener |
|------------------------------------|--|-------------------|----------------------|
| Density (g/cc) | 2.52 | 1.14 | 1.19 |
| Tensile strength (MPa) | 3.31 | 73.3 | 52 |
| Modulus of elasticity (GPa) | 72.4 | 3.47 | 2.8 |
| Elongation (%) | 4.8 | 4.5 | 11 |
| Nano fillers | Titanium dioxide (TiO_2) | Graphene | |
| Molar mass (g/mol) | 79.866 | 12.01 | |
| Density (kg/m ³) | 4.23 | 2.267 | |
| Melting point (°C) | 1843 | 3652–3697 | |
| Boiling point (°C) | 2972 | 4200 | |

Table 1. Constituent properties of materials used in the study.

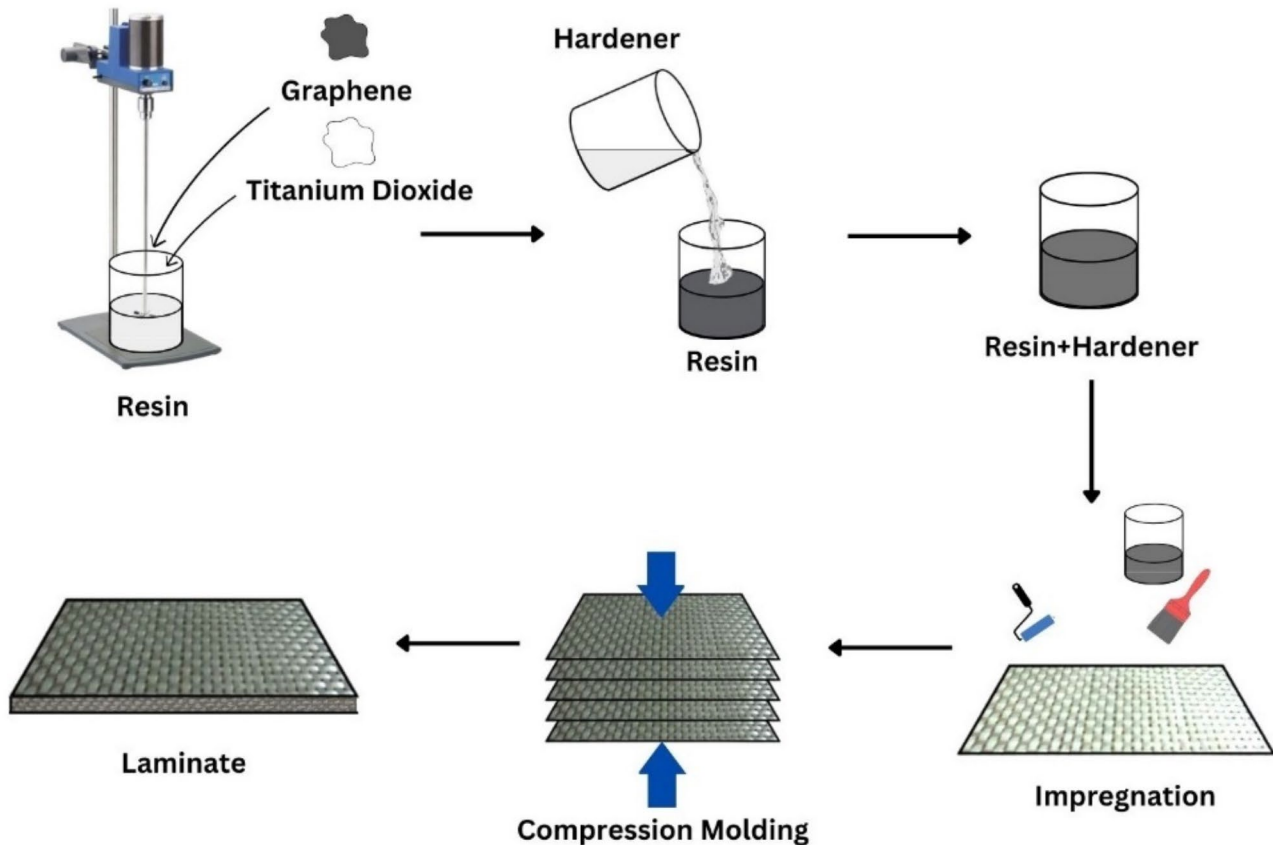


Fig. 1. Fabrication method of fiber glass/epoxy nanocomposites.

A roller was used to spread the resin mixture evenly and avoid any air bubbles between the fabric layers. Finally, the composite was cured at a pressure of 5 bar for 4 h at room temperature. This nanocomposite with a total wt% of 1% was designated as GT1. The fabrication process of the nanocomposite is detailed in Fig. 1. The process was repeated with a total wt% of 2 wt%, 3 wt%, and 4 wt% of the fillers and fabricated nanocomposites were designated as GT2, GT3, and GT4, respectively. A fiberglass/epoxy composite without any nanofiller was also fabricated and designated as GT0.

Drilling

Drilling of the fabricated nanocomposites was performed using the 4-axis CNC vertical machine setup equipped with a milling tool dynamometer located at Madras Institute of Technology (MIT), Chennai, India. Carbide coated drill bits dominate in enhancing machining performance by reducing thrust force during drilling comparing with uncoated bits²¹. As a result, carbide coated high-speed steel drill bits with diameters of 4 mm, 6 mm, and 8 mm were used in this research. Glass fiber composites can be drilled at as high speeds as 10,000 rpm and at higher feed rates of 200 mm/min but drilling at high rpm increases delamination and high feed rates increase thrust force reducing quality of the hole. As a result, rpm of 600–1800 rev/min and feed rate of 30–

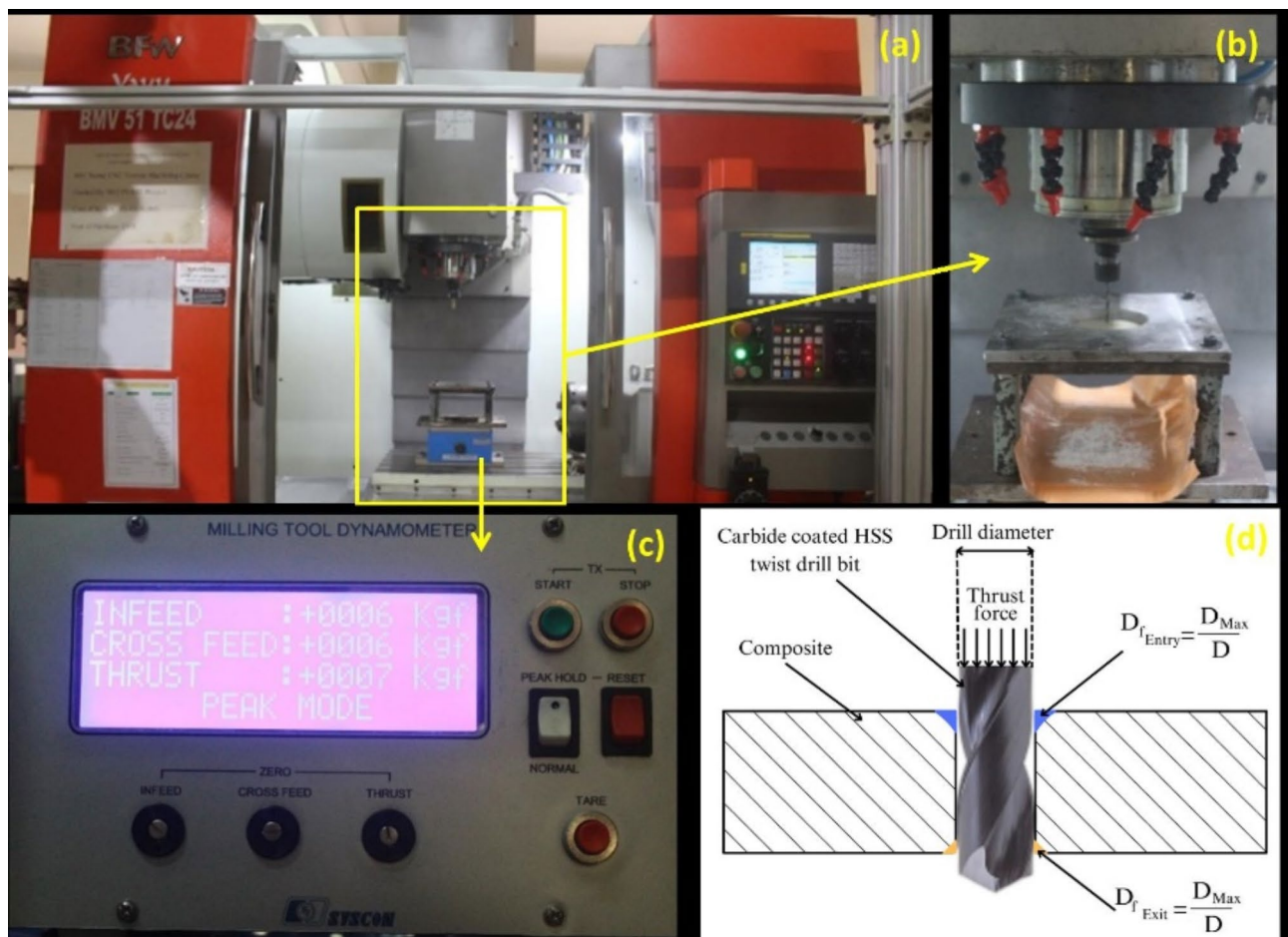


Fig. 2. Drilling setup and performance metrics.

| Factors | Levels | Values |
|--|--------|--------------------------|
| Filler % | 5 | 0, 1, 2, 3, 4 |
| Diameter (mm) | 3 | 4, 6, 8 |
| Spindle speed (rpm)/Feed rate (mm/min) | 3 | 600/30, 1200/40, 1800/50 |

Table 2. Drilling parameters.

50 mm/min were considered in this study^{22,23}. A custom fixture was used to hold the composite plate in place during the drilling process, as shown in Fig. 2. The fixture was attached to a strain gauge-based mechanical sensing unit of Syscon milling tool dynamometer. A digital force indicator is attached to the dynamometer to monitor the thrust force exerted during the drilling process. Peak mode was selected on the equipment to obtain the maximum thrust force during the process.

The process parameters for the experiment are shown in Table 2.

Assessment of delamination

Entry and exit faces of drilled holes were photographed using a high-resolution Sony 4k camera with a 26.8–536 mm focal length, 3.8 mm maximum aperture and 20× optical zoom. MATLAB was used for image processing as described by da Silva et al.²⁴. Raw images were converted from color to monochromatic using MATLAB in which the damaged area was assigned black color with a binary value of 0 while the undamaged area was given a white color with a binary value of 1. These binary values were stored in the form of arrays for image processing. Monochromatic images were filtered removing black regions that were not drilling-induced using threshold of binary values obtained from histogram data of image near delaminated area resulting in a final image. This final image was compared to the original image to ensure accurate image subtraction was achieved. The pixels of inner and outer diameter of the damaged area were calculated from MATLAB and delamination factor was obtained by dividing pixels of outer diameter by pixels of inner diameter as shown in Fig. 3. The process was repeated at all the entry and exit faces of the holes drilled.

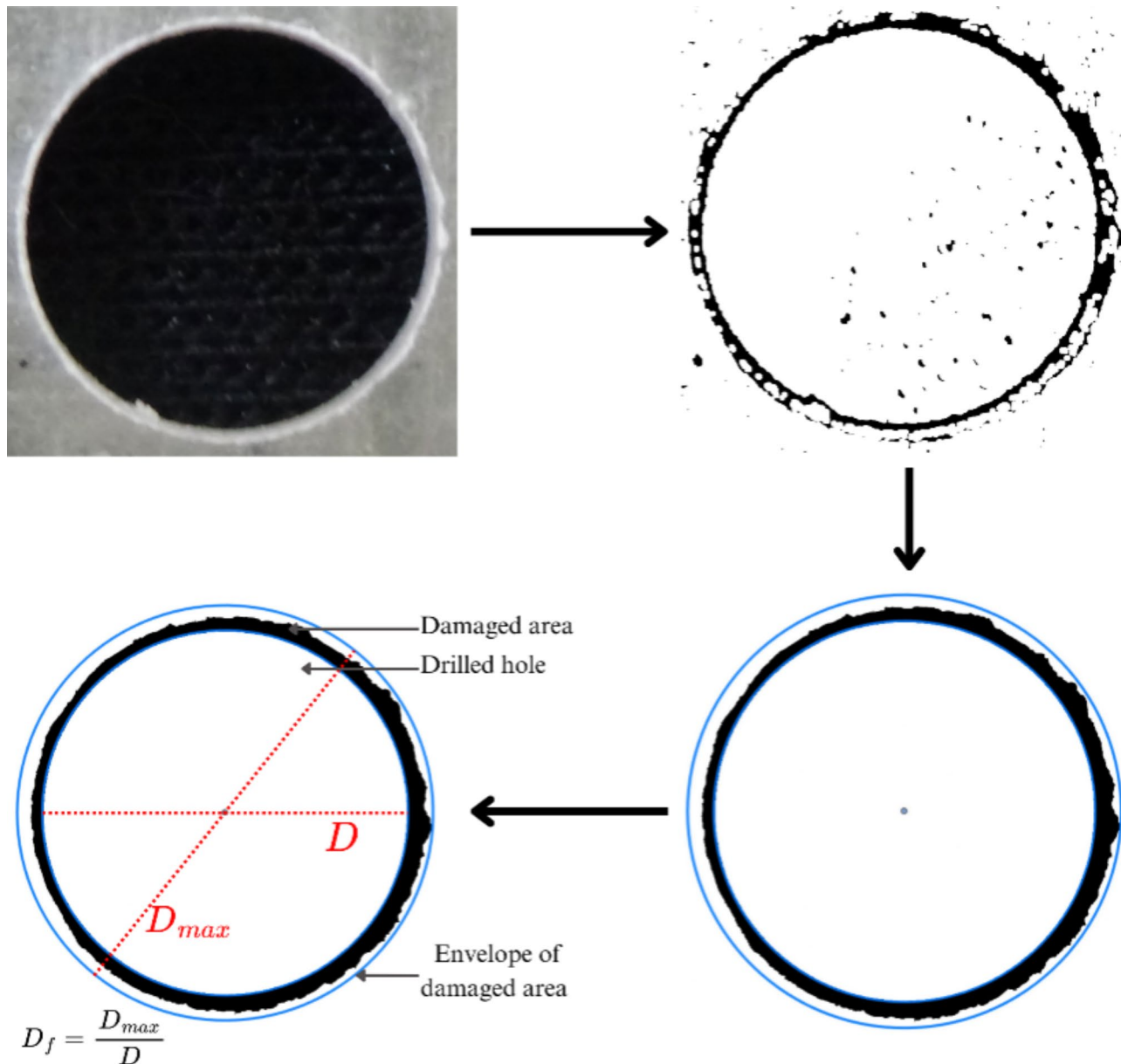


Fig. 3. Image processing in MATLAB.

Grey relational analysis

Grey relational analysis is a multivariate statistical technique used to convert multi response variables into a single response known as Grey Relational Grade (GRG). Comparing with other optimization techniques which optimize only one response at a time, Grey relational analysis optimizes multiple response variables at a time even with poor or insufficient information and often preferred in finding optimum machining parameters of composites²⁵. The data can be normalized using different methods to eliminate different ranges and units in the data sequence²⁶.

The normalization of data sequence can be done as “lower is better” when a lower output response is desired using:

$$x_i^*(k) = \frac{\max_{\forall i} x_i^o(p) - x_i^o(p)}{\max_{\forall i} x_i^o(p) - \min_{\forall i} x_i^o(p)} \quad (1)$$

If “nominal is better”, then:

$$x_i^*(k) = \frac{x_i^0(p) - x_i^0}{\max_{\forall i} x_i^0(p) - x_i^0(p)} \quad (2)$$

If “higher is better”, then:

$$x_i^*(k) = \frac{x_i^0(p) - \min_{\forall i} x_i^0(p)}{\max_{\forall i} x_i^0(p) - \min_{\forall i} x_i^0(p)} \quad (3)$$

where $x_i^0(p)$ is the original data sequence, $x_i^*(p)$ is the normalized sequence and i is the n -th number of results of p -th response factor.

In machining thrust force and delamination are desired to be lower to enhance hole quality as a result lower the better was selected to normalize thrust force, delamination at entry and exit. The normalized sequence can be used to express the relationship with the ideal experimental results through Grey Relation Coefficient. The grey relation coefficient is determined using the following equation:

$$\xi(p) = \frac{\Delta_{min} + \zeta \Delta_{max}}{\Delta_{0i}(p) + \zeta \Delta_{max}} \quad (4)$$

$$\Delta_{0i}(p) = \|x_0^*(p) - x_i^*(p)\| \quad (5)$$

$$\Delta_{min} = \left(\frac{\min}{\forall j \in i} \right) \left(\frac{\min}{\forall p} \right) \|x_0^*(p) - x_j^*(p)\| \quad (6)$$

$$\Delta_{max} = \left(\frac{\max}{\forall j \in i} \right) \left(\frac{\max}{\forall p} \right) \|x_0^*(p) - x_j^*(p)\| \quad (7)$$

where Δ_{0i} is the absolute difference between $x_0^*(p)$ and $x_i^*(p)$, in other words, called a deviation sequence and ζ is the distinguishing coefficient ranging between 0 and 1.

GRG is the average of each sequence's grey relational coefficient. It is computed using:

$$\gamma_i = \frac{1}{n} \sum_{p=1}^n \xi_i(p) \quad (8)$$

However, many factors influence significant factors, and they vary accordingly. As a result, Eq. (9) can be used to calculate the grey relational grade value.

$$\gamma_i = \frac{1}{n} \sum_{p=1}^n w_p \xi_i(p) \quad (9)$$

where w_p is normalized weight for the factor p . All factors were considered equal in this problem as a result Eq. (8) was used to calculate grey relational grade.

Results and discussions

Thrust force, delamination at entry and exit obtained from drilling nanocomposites at different drilling parameters were depicted in Table 3. A detailed explanation of results obtained from experiments were discussed in the following sections.

Morphological analysis

Quality of hole is one of the factors assessed after drilling the composites. Studying the surface morphology of the drilled holes, the quality of the holes can be examined. Figure 4. shows the morphological images of the top and rear face of the drilled holes. Matrix smearing and uncut fibers were observed on entry and exit faces. Higher amounts of uncut fiber were observed at the rear face comparing with the entry face. According to Çelik et al.²⁷, heat accumulation at the tip of the drill bit softens the matrix in the composite at low feed rates and higher spindle speeds, causing matrix smearing. This heat accumulation is due to the low coefficient of thermal conductivity of glass, which leads to an increase in temperature at the drilling surface. An increase in feed rate causes the fiber not to cut properly, leading to uncut fibre. Khashaba et al.²⁸ work states that the cause of uncut fibers is due to the fact that the drill point acts as a punch at higher feed rates that pierces the laminate instead of cutting through it. According to Kavad et al.²⁹, feed rate, tool material, and cutting speed are the most influential factors on the delamination factor in conventional machining, and they conclude that higher speed, harder tool material, and a lower feed rate achieve low delamination damage.

Analysis of thrust force

Thrust force obtained by drilling GT0-GT4 nanocomposites at different drilling parameters were depicted in Fig. 5. A higher thrust force of 98.1 N was observed in GT4 with a 6 mm bit at 600 RMP and 30 mm/min comparing with other nanocomposites whereas lower thrust force of 19.62 N was observed in GT2 and GT4

| Trial no. | Specimen | Drill bit diameter (mm) | Spindle speed (rpm) | Feed rate (mm/min) | Thrust (N) | D_f Entry | D_f Exit |
|-----------|----------|-------------------------|---------------------|--------------------|------------|-------------|------------|
| 1 | GT0 | 4 | 600 | 30 | 39.24 | 1.33466 | 1.1084 |
| 2 | | | 1200 | 40 | 39.24 | 1.20344 | 1.0918 |
| 3 | | | 1800 | 50 | 29.43 | 1.29782 | 1.13774 |
| 4 | | 6 | 600 | 30 | 68.67 | 1.17457 | 1.14946 |
| 5 | | | 1200 | 40 | 49.05 | 1.19956 | 1.16526 |
| 6 | | | 1800 | 50 | 29.43 | 1.21794 | 1.20655 |
| 7 | | 8 | 600 | 30 | 58.86 | 1.22451 | 1.14419 |
| 8 | | | 1200 | 40 | 49.05 | 1.22372 | 1.14887 |
| 9 | | | 1800 | 50 | 39.24 | 1.2043 | 1.17079 |
| 10 | GT1 | 4 | 600 | 30 | 49.05 | 1.2321 | 1.07329 |
| 11 | | | 1200 | 40 | 29.43 | 1.28025 | 1.12581 |
| 12 | | | 1800 | 50 | 29.43 | 1.2403 | 1.08661 |
| 13 | | 6 | 600 | 30 | 58.86 | 1.1565 | 1.15332 |
| 14 | | | 1200 | 40 | 39.24 | 1.14463 | 1.10698 |
| 15 | | | 1800 | 50 | 29.43 | 1.22717 | 1.16589 |
| 16 | | 8 | 600 | 30 | 78.48 | 1.24344 | 1.16509 |
| 17 | | | 1200 | 40 | 58.86 | 1.23003 | 1.18517 |
| 18 | | | 1800 | 50 | 49.05 | 1.20399 | 1.16727 |
| 19 | GT2 | 4 | 600 | 30 | 49.05 | 1.29725 | 1.15789 |
| 20 | | | 1200 | 40 | 29.43 | 1.24412 | 1.12207 |
| 21 | | | 1800 | 50 | 19.62 | 1.30233 | 1.11253 |
| 22 | | 6 | 600 | 30 | 68.67 | 1.22377 | 1.15558 |
| 23 | | | 1200 | 40 | 58.86 | 1.199 | 1.18424 |
| 24 | | | 1800 | 50 | 29.43 | 1.15694 | 1.12405 |
| 25 | | 8 | 600 | 30 | 78.48 | 1.15688 | 1.13512 |
| 26 | | | 1200 | 40 | 58.86 | 1.18954 | 1.14592 |
| 27 | | | 1800 | 50 | 49.05 | 1.17724 | 1.15794 |
| 28 | GT3 | 4 | 600 | 30 | 39.24 | 1.27617 | 1.07752 |
| 29 | | | 1200 | 40 | 29.43 | 1.27191 | 1.17633 |
| 30 | | | 1800 | 50 | 29.43 | 1.18366 | 1.23129 |
| 31 | | 6 | 600 | 30 | 58.86 | 1.18684 | 1.21905 |
| 32 | | | 1200 | 40 | 49.05 | 1.21808 | 1.18462 |
| 33 | | | 1800 | 50 | 29.43 | 1.18509 | 1.18647 |
| 34 | | 8 | 600 | 30 | 78.48 | 1.16867 | 1.14571 |
| 35 | | | 1200 | 40 | 49.05 | 1.20532 | 1.18721 |
| 36 | | | 1800 | 50 | 49.05 | 1.19024 | 1.18182 |
| 37 | GT4 | 4 | 600 | 30 | 29.43 | 1.40401 | 1.08785 |
| 38 | | | 1200 | 40 | 29.43 | 1.28946 | 1.05875 |
| 39 | | | 1800 | 50 | 19.62 | 1.30521 | 1.16154 |
| 40 | | 6 | 600 | 30 | 98.1 | 1.26015 | 1.26788 |
| 41 | | | 1200 | 40 | 88.29 | 1.2577 | 1.25796 |
| 42 | | | 1800 | 50 | 49.05 | 1.30339 | 1.25505 |
| 43 | | 8 | 600 | 30 | 88.29 | 1.27618 | 1.24813 |
| 44 | | | 1200 | 40 | 58.86 | 1.24125 | 1.19289 |
| 45 | | | 1800 | 50 | 49.05 | 1.27379 | 1.2325 |

Table 3. Results from the experiment.

with 4 mm bit at 1800 rpm and 50 mm/min comparing with other composites. GT1 and GT2 showed similar results of thrust force with a higher thrust force of 78.48 N with 8 mm drill bit at 600 rpm and 30 mm/min feed rate comparing with other nanocomposites. Two different trends were noticed in the thrust plot. The first trend was a declining thrust force with the increase in spindle speed and feed rate for similar diameter of the hole drilled irrespective of the filler percentage. According to Anand et al.³⁰, the tool becomes thermally soft with an increase in spindle speed facilitating the easy flow of chips from the material, resulting in lower thrust force. The second trend was an increase in thrust force with the increase in drill bit diameter. These observations align with the trends reported in the literature on composite laminates^{31,32}. A similar trend in thrust force was observed in research performed by Mohan et al.³³ validating the influence of drilling parameters on thrust force obtained in this study.

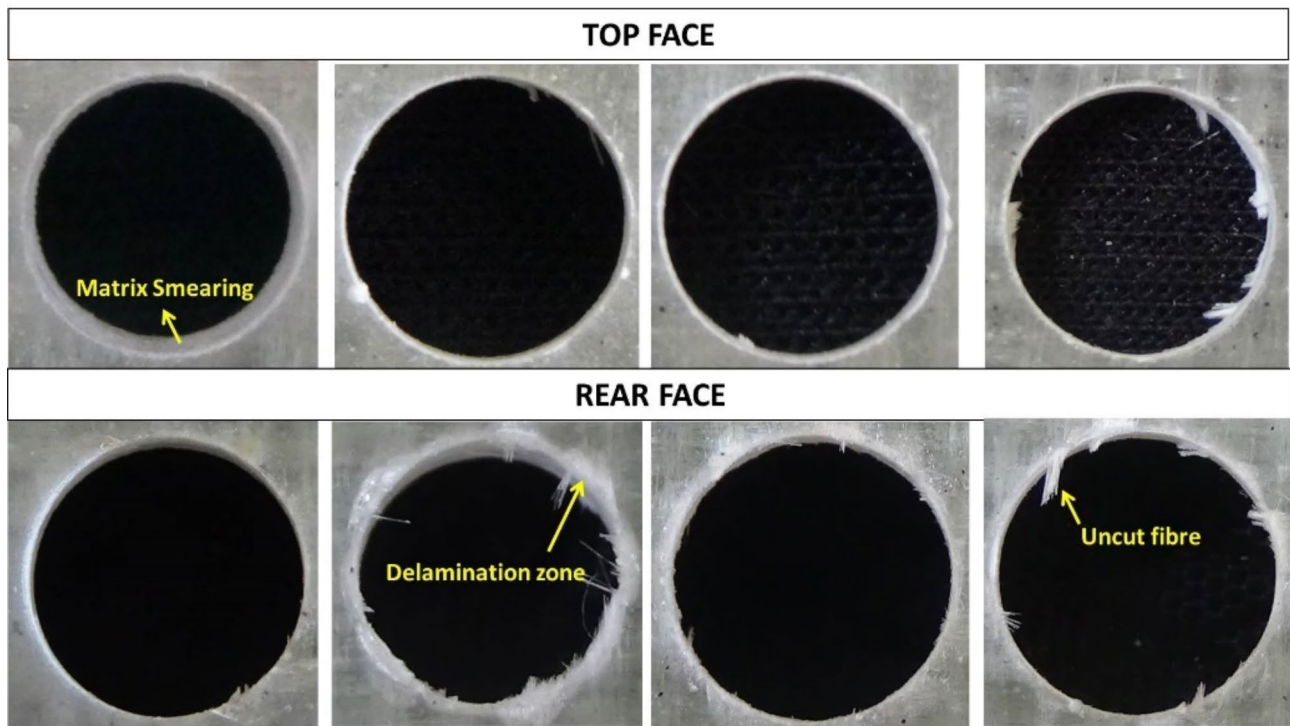


Fig. 4. Morphological images of the drilled holes.

Thrust force mapping was done as shown in Fig. 6 to assess the influence of filler on the thrust force while drilling nanocomposites. It is evident from the color codes in the mapping that the presence of nanofillers in smaller proportions does not affect the drilling process. Only a marginal variation of thrust force could be observed for the GT1–GT3. Whereas GT4, with higher wt% of fillers showed maximum thrust force with notable variation at different spindle speeds and feed rates indicating presence of nanofiller in higher proportions, along with spindle speed and feed rate generated higher thrust force influencing the drilling process. Another interesting observation from the thrust force map is the significant variation in thrust force between the different hole diameters, where an increasing magnitude of thrust force was observed with the increasing hole diameter.

Analysis of delamination

Maximum delamination at entry was observed in GT4 with 4 mm drill bit at spindle speed of 600 rev/min and 30 mm/min feed rate. Delamination at entry, which is 18.47% lower comparing with GT4 was observed in GT1 with 6 mm drill bit at 1200 rev/min and 40 mm/min. Minimum delamination at exit was observed in GT4 with 4 mm drill bit at 1200 rev/min and 40 mm/min feed rate. Higher delamination at exit was also observed in GT4 with an increase of 16.49% with 6 mm drill bit at 600 rev/min and feed rate of 30 mm/min. Contour plots showing the influence of spindle speed and drill bit diameter on delamination factors at entry and exit were shown in Fig. 7. This contour visualization was useful to evaluate the combination of inputs where minimum delamination can be achieved.

Delamination at entry and exit of the GT0 was consistent with the works of Mohan et al.⁵ and Kilickap et al.³⁴, which stated an increase in delamination with an increase in cutting parameters. The presence of nanofillers evidently had effects on the delamination factor. GT1 showed the least amount of delamination at entry at a 6 mm drill bit and 1200 rpm spindle speed. GT2 achieved lower delamination across different drill bit diameters and spindle speeds compared to other specimens. GT4 showed the highest delamination overall across the 4 mm and 6 mm drill bit diameters and the lowest spindle speeds of 600 rpm. According to Ragunath et al.³⁵, at higher filler % the strength of the composite reduces resulting in an increased delamination this also agrees with El-Ghaoui, Khalid et al.¹⁵.

ANOVA analysis

Analysis of variance (ANOVA) is a statistical tool used to evaluate whether an input has a significant effect on the response of the experiment. ANOVA factor information was given in Table 4.

From the ANOVA analysis, the following empirical models of outputs were achieved for factors in Table 4:

$$\begin{aligned} \text{Thrust} = & 48.61 - 3.92 A_0 - 1.74 A_1 + 0.44 A_2 - 2.83 A_3 + 8.07 A_4 - 15.91 B_0 + 5.01 B_1 \\ & + 10.90 B_2 + 14.17 C_0 - 0.87 C_1 - 13.30 C_2 \end{aligned}$$

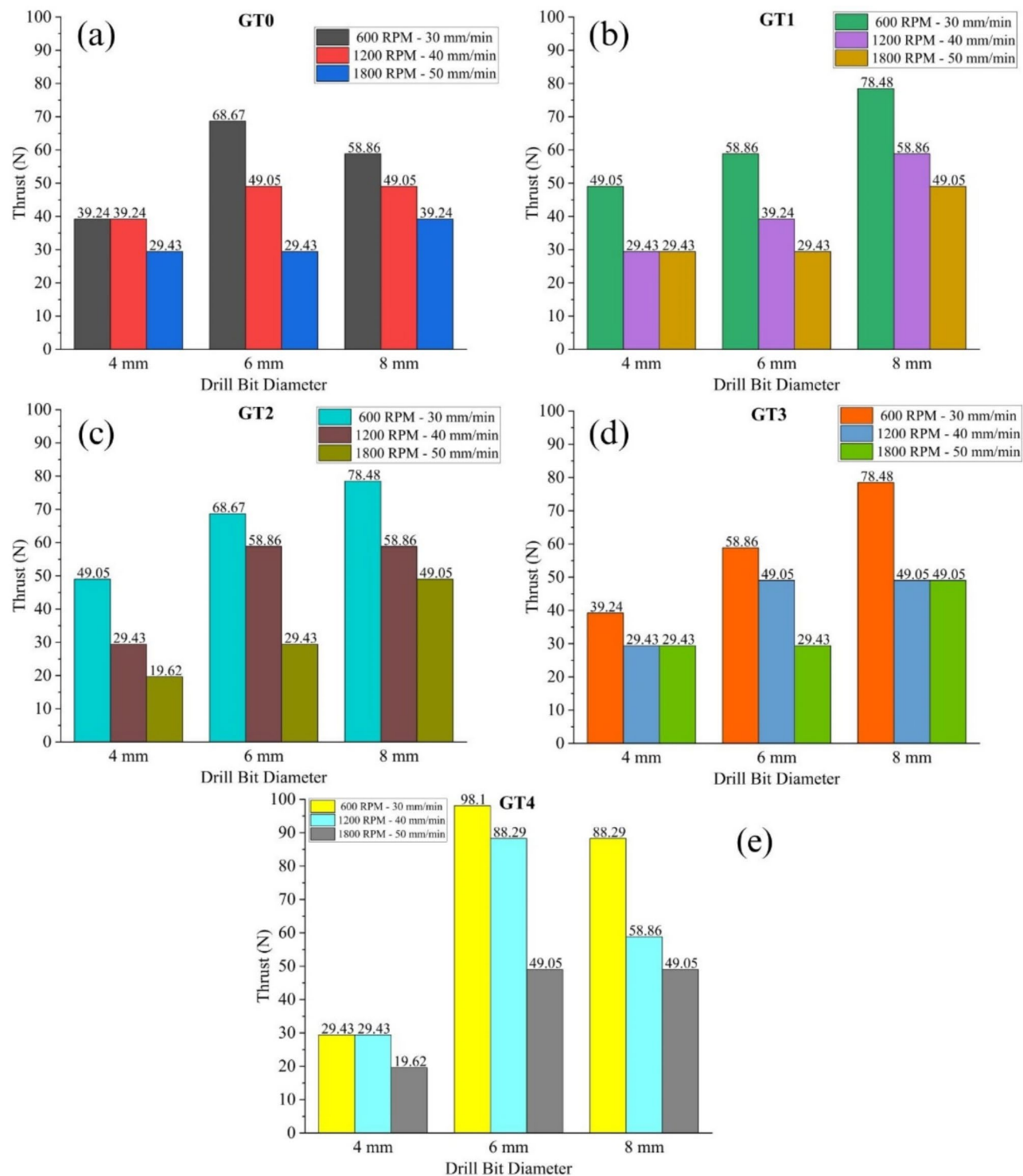


Fig. 5. Thrust force for glass/epoxy composites (a) GT0, (b) GT1, (c) GT2, (d) GT3 & (e) GT4.

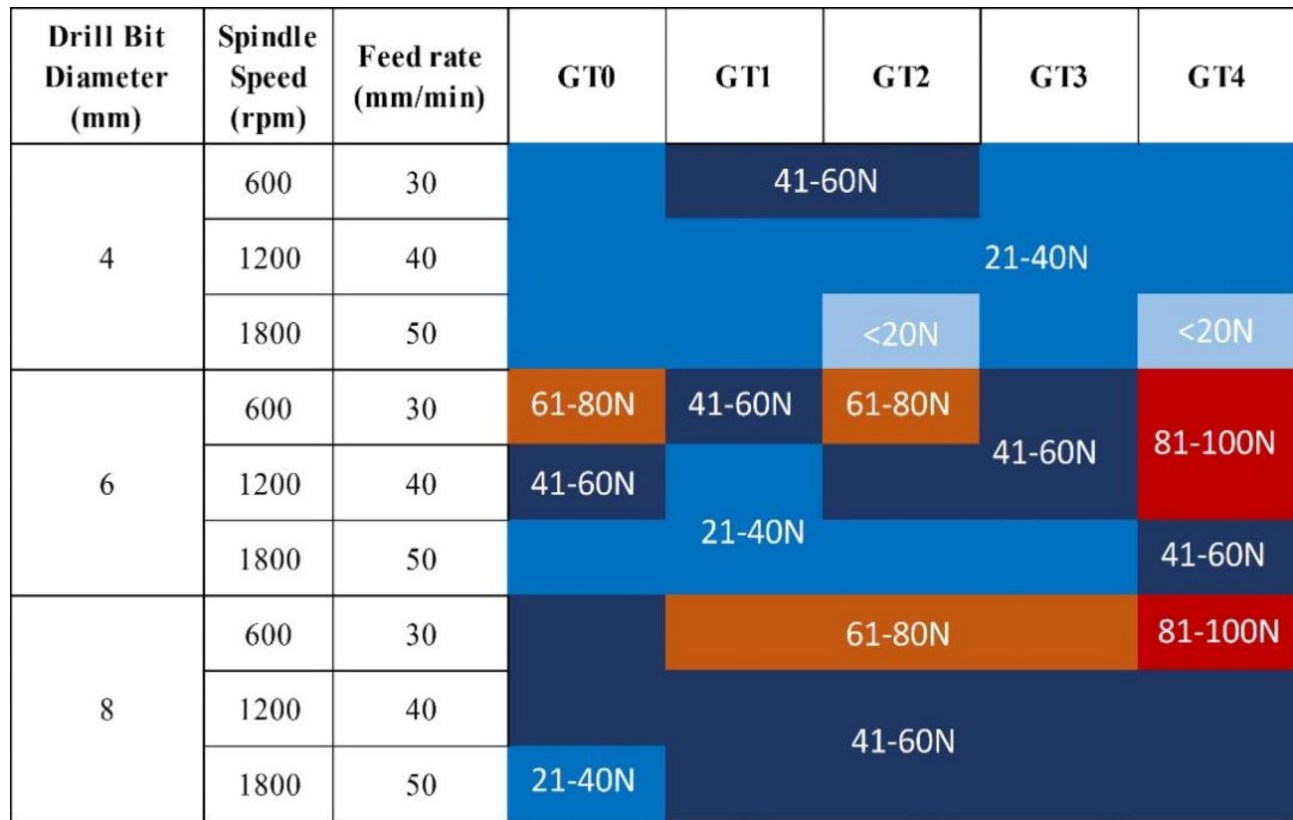


Fig. 6. Mapping of thrust force for GT0–GT4.

$$D_f \text{ Entry} = 1.23296 - 0.0018 A_0 - 0.0154 A_1 - 0.0166 A_2 - 0.0234 A_3 + 0.0572 A_4 + 0.04455 B_0 - 0.02554 B_1 - 0.01902 B_2 + 0.00809 C_0 - 0.00642 C_1 - 0.00166 C_2$$

$$D_f \text{ Exit} = 1.16001 - 0.0130 A_0 - 0.0234 A_1 - 0.0161 A_2 + 0.0167 A_3 + 0.0358 A_4 - 0.03938 B_0 + 0.02548 B_1 + 0.01390 B_2 - 0.00744 C_0 - 0.00442 C_1 + 0.01186 C_2$$

Table 5 depicts the output of the general linear ANOVA model carried out in Minitab with a significance level of $P \leq 0.05$. If the $P > 0.05$, then null hypothesis is true, which means that there is no statistical difference between the group mean. If the $P \leq 0.05$, then null hypothesis is rejected, which means that there is statistical difference between the group mean. If the $F < 4$, then the parameter does not have significance on the output⁵.

Drill bit diameter showed 36.44% contribution on thrust force and spindle speed/feed rate contributed 34.71% to thrust force showing their significance on thrust force whereas filler % contributed only 5.05% showing filler % does not have any influence on thrust force. Filler % showed significant influence on delamination at entry and exit. Filler % contributed 30.05% to delamination at entry and 20.22% to delamination at exit. As delamination is dependent on mechanical properties of the composite adding fillers alter the mechanical properties of composites showing significant influence of filler % on delamination at entry and exit³⁶. Drill bit diameter contributed 34.68% to delamination at entry whereas it contributed 31.80% to delamination at exit showing its significance. The effects of spindle speed/feed rate were insignificant on delamination at entry and exit with a contribution of < 3% which aligns with the research done by Krishnaraj et al.³⁷.

Analysis of results using signal-to-noise ratio (S/N)

Quality of the obtained output value deviating from the desired value is measured using S/N ratio. Process parameters with higher S/N ratios have optimum quality with minimum variance. Mean S/N ratio and the main effects plot for GT0–GT4 at different levels of drilling parameters were provided in Table 6; Fig. 8, respectively. “Smaller the better” quality characteristic was applied for both thrust force and delamination factors. The minimum thrust force was considered ideal since an increase in thrust force causes an increase in delamination. Thrust force and delamination at the top face ($D_f \text{ Entry}$) and delamination at the rear face ($D_f \text{ Exit}$) were converted to a signal-to-noise (S/N) ratio using the “smaller-the-better” characteristic with the following equation:

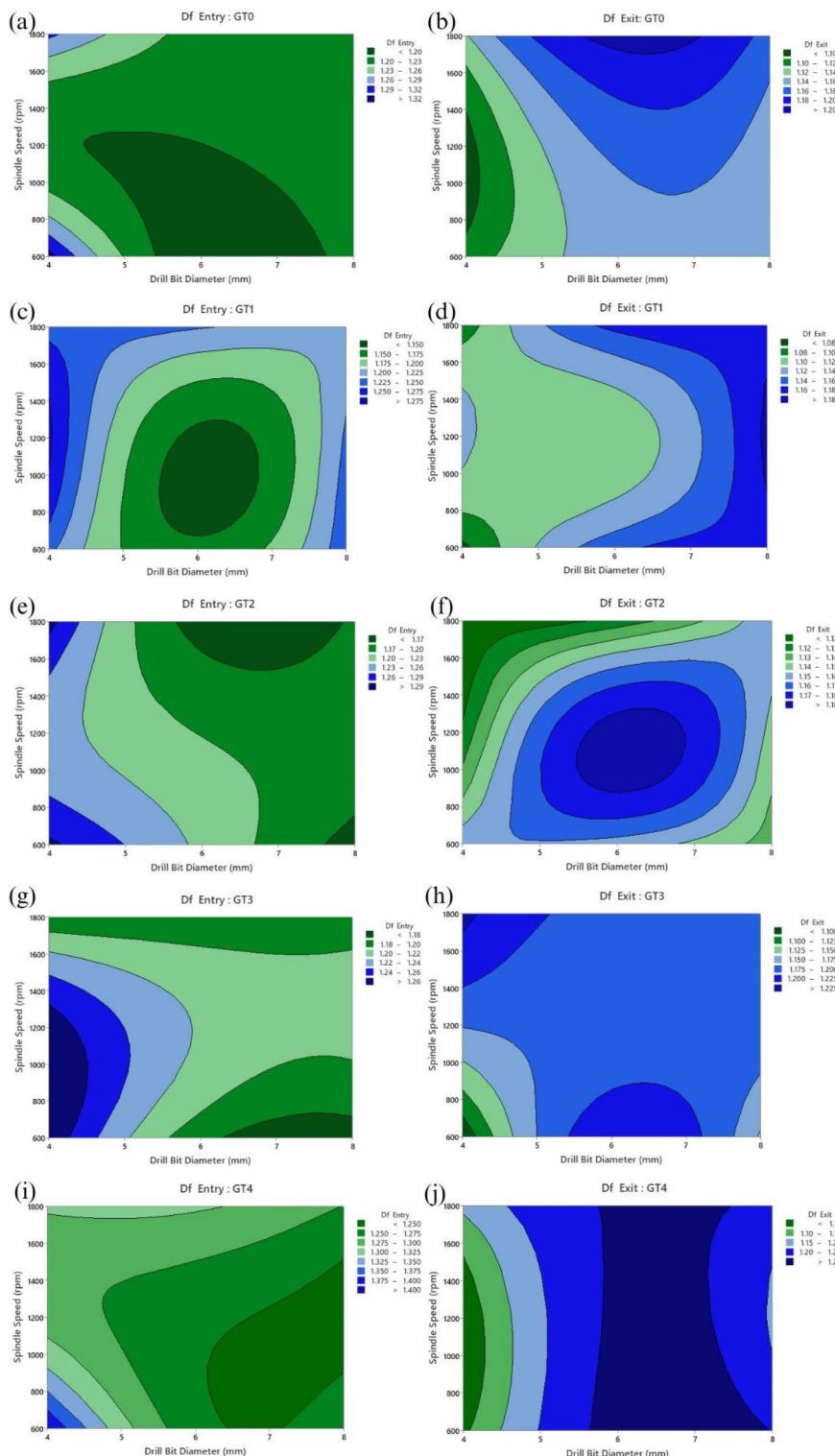


Fig. 7. Contour plots for D_f Entry & D_f Exit.

$$S/N \text{ ratio} = -10 \log_{10} \left(\frac{1}{n} \sum_{i=1}^n z_{ij}^2 \right) \quad (10)$$

here z_{ij} is measured response value, $i = 1, 2, 3 \dots n$; $j = 1, 2, 3 \dots k$ and n are number of replications.

Figure 8a shows drill bit diameter, spindle speed/feed rate had a larger influence on the thrust force, whereas the nanofiller proportion in the composites had negligible influence which was also observed in the ANOVA.

| Factor | Notation | Levels | Values | | | | |
|-----------------------------|----------|--------|-------------------|--------------------|--------------------|----|----|
| | | | 0 | 1 | 2 | 3 | 4 |
| Filler % | A | 5 | 0% | 1% | 2% | 3% | 4% |
| Drill bit diameter | B | 3 | 4 mm | 6 mm | 8 mm | — | — |
| Spindle speed/ feed rate | C | 3 | 600 rpm/30 mm/min | 1200 rpm/40 mm/min | 1800 rpm/50 mm/min | — | — |

Table 4. ANOVA factor information.

| Source | DF | Contribution | Adj SS | Adj MS | F-value | P-value | Inference |
|---|----|--------------|---------|--------|--------------------------------|------------|-----------------|
| Thrust Force | | | | | | | |
| A | 4 | 5.05% | 825.5 | 206.4 | 1.91 | 0.13013414 | Not significant |
| B | 2 | 36.44% | 5958.1 | 2979 | 27.55 | 0.00000006 | Significant |
| C | 2 | 34.71% | 5675.8 | 2837.9 | 26.25 | 0.00000009 | Significant |
| Error | 36 | 23.80% | 3892.2 | 108.1 | | | |
| Total | 44 | 100.00% | 16351.6 | | | | |
| S = 10.3979 | | | | | R ² = 76.20% | | |
| Predicted residual error of sum of square (PRESS) = 6081.59 | | | | | R ² (adj) = 70.91% | | |
| | | | | | R ² (pred) = 62.81% | | |
| D _f Entry | | | | | | | |
| A | 4 | 30.05% | 0.0389 | 0.0097 | 7.95 | 0.000105 | Significant |
| B | 2 | 34.68% | 0.0449 | 0.0224 | 18.36 | 0.000003 | Significant |
| C | 2 | 1.27% | 0.0016 | 0.0008 | 0.67 | 0.517868 | Not significant |
| Error | 36 | 34.00% | 0.0441 | 0.0012 | | | |
| Total | 44 | 100.00% | 0.1297 | | | | |
| S = 0.0350008 | | | | | R ² = 66% | | |
| Predicted residual error of sum of square (PRESS) = 0.0689095 | | | | | R ² (adj) = 58.44% | | |
| | | | | | R ² (pred) = 46.87% | | |
| D _f Exit | | | | | | | |
| A | 4 | 20.22% | 0.0228 | 0.0057 | 4.03 | 0.008366 | Significant |
| B | 2 | 31.80% | 0.0358 | 0.0179 | 12.69 | 0.000067 | Significant |
| C | 2 | 2.86% | 0.0032 | 0.0016 | 1.14 | 0.330277 | Not significant |
| Error | 36 | 45.11% | 0.0509 | 0.0014 | | | |
| Total | 44 | 100.00% | 0.1128 | | | | |
| S = 0.0376138 | | | | | R ² = 54.89% | | |
| Predicted residual error of sum of square (PRESS) = 0.0795824 | | | | | R ² (adj) = 44.86% | | |
| | | | | | R ² (pred) = 29.51% | | |

Table 5. ANOVA results for thrust force, delamination at entry and exit.

Drill bit of 4 mm resulted in lower thrust values with high S/N ratio suggesting lower drill bit diameter is preferred. S/N ratio for thrust force at spindle speed of 1800 rev/min is high showing high spindle speeds reduce thrust force which is true according to Anand et al.³⁰. Filler % did not show any significant changes in S/N ratio of thrust force showing its insignificance. However, the presence of nanofiller at different proportions was found to have a significant impact on the delamination ($D_{f\text{Entry}}$ and $D_{f\text{Exit}}$) which are evident in Fig. 8b,c. Drill bit was the most influencing parameter among all the drilling parameters as indicated by higher gradient in S/N ratio over other parameters. In the case of delamination, spindle speed and feed rate had only marginal influence. Responses of each level of drilling parameters on the delamination at entry and delamination at exit were opposite to each other as observed from the gradient of S/N ratio. For instance, increasing the drill bit diameter, spindle speed, and feed rate had a negative influence, leading to an increase in delamination at entry and vice versa for delamination at exit. These observations corroborate a recent study published on fiberglass/epoxy nanocomposites reinforced with carbon nanotubes³⁸. According to them, the penetration action of the chisel edge of the drill bit tends to extrude the nanocomposite rather than cutting under the increasing feed rate and spindle speed, thus increasing the delamination area.

Analysis of results using grey relation

Grey Relational Grade (GRG) determined for GT0–GT4 for the various levels of drilling parameters was depicted in Table 7. Depending on the GRG value, a rank was given for every trial. Rank of 1 is given to the trial

| Description | Level | Filler % | Drill bit diameter | Spindle speed & feed rate |
|--------------|-------|----------|--------------------|---------------------------|
| Thrust force | 1 | -32.6814 | -29.9976 | -35.5232 |
| | 2 | -32.9239 | -33.9485 | -33.1338 |
| | 3 | -33.0727 | -35.2627 | -30.5518 |
| | 4 | -32.7480 | - | - |
| | 5 | -33.9219 | - | - |
| D_f Entry | 1 | -1.7998 | -2.1202 | -1.8631 |
| | 2 | -1.7052 | -1.6320 | -1.7695 |
| | 3 | -1.6933 | -1.6805 | -1.8000 |
| | 4 | -1.6485 | - | - |
| | 5 | -2.2076 | - | - |
| D_f Exit | 1 | -1.1880 | -0.9825 | -1.2235 |
| | 2 | -1.1074 | -1.4713 | -1.2487 |
| | 3 | -1.1665 | -1.3897 | -1.3712 |
| | 4 | -1.4074 | - | - |
| | 5 | -1.5365 | - | - |

Table 6. Mean S/N ratio of GT0–GT4.

with higher GRG values. Every specimen was ranked individually among its own filler group for GT0–GT4 and an overall rank considering all experimental iterations for GT0–GT4 was also tabulated in Table 7. According to the overall rank of the grey relation analysis, the combination of GT1, 6 mm drill bit diameter at 1200 rpm spindle speed, and 40 mm/min produced the best response.

In order to evaluate the influence of various levels of drilling parameters, the mean GRG values were determined by using “larger the better” formulation of S/N ratio and presented in Table 8; Fig. 9, respectively. It was apparent that the presence of nanofillers significantly improved multiple performance characteristics during drilling.

Among the process parameters, drill bit diameter was most influential, followed by filler (%) and spindle speed, and feed rate. The highest value of mean GRG was obtained for the highest level of feed rate and spindle speed. Both D_f Entry and thrust force increased substantially with the increasing feed rate. This is because the drill point acts like a punch on the laminate, instead of cutting through it, causing more damage around the drilled hole³⁸. Based on Table 8, the optimum parameters for drilling glass/epoxy composites reinforced with TiO_2 and graphene were as follows:

- Nanofiller at 1 wt%.
- Drill bit diameter of 4 mm.
- Spindle speed and feed rate of 1800 rpm and 50 mm/min.

Conclusions

Effects of drilling fiberglass/epoxy composites reinforced with TiO_2 and graphene from 1 to 4 wt% at different drilling parameters on thrust force and delamination at entry/exit were investigated in this study. Taguchi-based grey relational analysis approach was applied to find optimum drilling parameters. ANOVA was performed to analyze the significance of different drilling parameters on machining nanocomposites. The following are the conclusions from this study:

- A 25% decrease in thrust force was observed with an increase in the spindle speed/feed rate irrespective of filler % and drill bit diameter.
- Glass fiber composite reinforced with 2 wt% & 4 wt% of titanium dioxide and graphene resulted in minimum thrust value of 19.62 N which is 33.3% lower comparing with thrust value of 29.43 N in nanocomposites reinforced with 1 wt% & 3 wt%.
- Increase in drill bit diameter resulted in a minimum increase of thrust force by 16.67% irrespective of other drilling parameters and filler %.
- Delamination at entry of GT1 was 18.47% lower comparing with GT4 whereas delamination at exit was lower in GT4.
- ANOVA indicated filler % contributed 30.05% for delamination at entry and 20.22% for delamination at exit showing its significance on delamination whereas it did not show any influence on thrust force.
- Spindle speed/feed rate had significant influence on thrust force whereas it did not show any significant influence on delamination.
- Drill bit diameter had significant influence on thrust force, delamination at entry and exit indicated by the steep gradient in mean effect plot of the S/N ratio.
- Considering all experiments conducted nanocomposite with 1 wt% when machined with 4 mm drill bit at 1800 rpm and feed rate of 50 mm/min resulted in optimum drilling parameters.

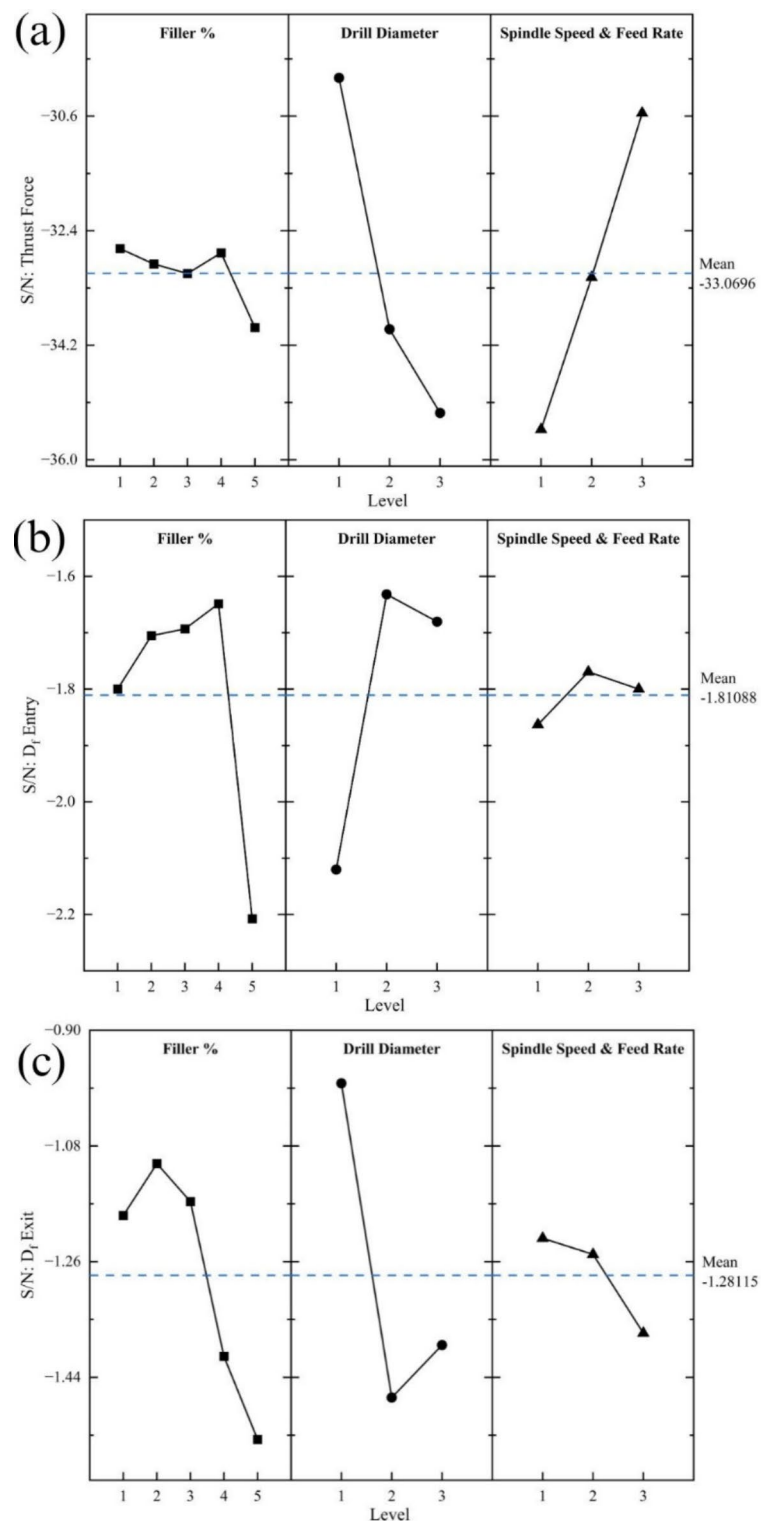
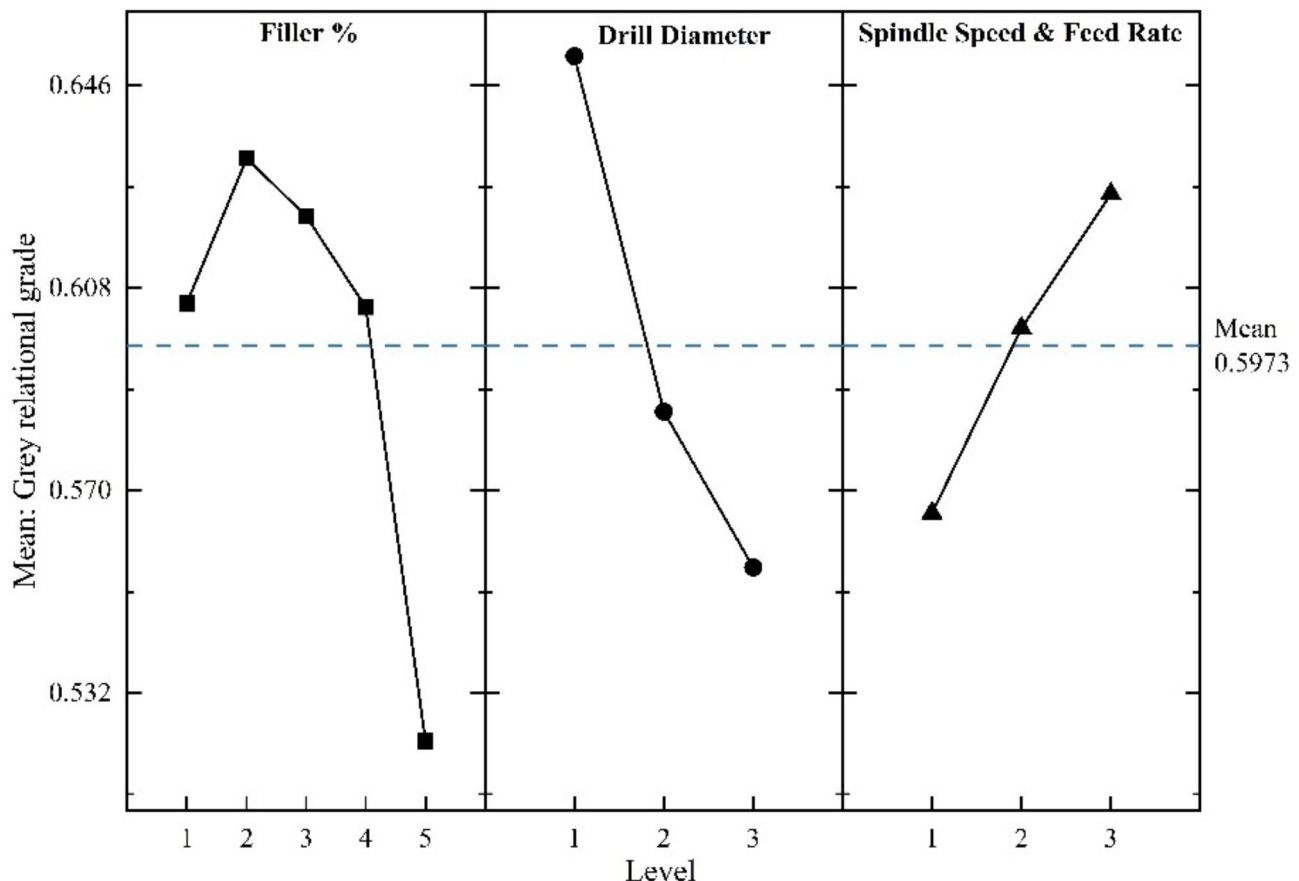


Fig. 8. Main effects plot for S/N ratio of GT0–GT4 (a) Thrust force, (b) D_f Entry and (c) D_f Exit.

| Trial no. | Normalization | | | Grey relation coefficient | | | Grey relation grade (GRG) | Rank | Overall rank |
|-----------|---------------|----------------------|---------------------|---------------------------|----------------------|---------------------|---------------------------|------|--------------|
| | Thrust | D _f Entry | D _f Exit | Thrust | D _f Entry | D _f Exit | | | |
| 1 | 0.7500 | 0.2674 | 0.7626 | 0.6667 | 0.4056 | 0.6780 | 0.5834 | 7 | 28 |
| 2 | 0.7500 | 0.7733 | 0.8420 | 0.6667 | 0.6880 | 0.7598 | 0.7048 | 1 | 5 |
| 3 | 0.8750 | 0.4094 | 0.6223 | 0.8000 | 0.4585 | 0.5697 | 0.6094 | 4 | 21 |
| 4 | 0.3750 | 0.8846 | 0.5663 | 0.4444 | 0.8124 | 0.5355 | 0.5975 | 5 | 22 |
| 5 | 0.6250 | 0.7882 | 0.4907 | 0.5714 | 0.7025 | 0.4954 | 0.5898 | 6 | 27 |
| 6 | 0.8750 | 0.7174 | 0.2932 | 0.8000 | 0.6389 | 0.4143 | 0.6177 | 2 | 19 |
| 7 | 0.5000 | 0.6920 | 0.5914 | 0.5000 | 0.6188 | 0.5503 | 0.5564 | 9 | 32 |
| 8 | 0.6250 | 0.6951 | 0.5690 | 0.5714 | 0.6212 | 0.5371 | 0.5766 | 8 | 30 |
| 9 | 0.7500 | 0.7699 | 0.4642 | 0.6667 | 0.6849 | 0.4827 | 0.6114 | 3 | 20 |
| 10 | 0.6250 | 0.6628 | 0.9305 | 0.5714 | 0.5972 | 0.8779 | 0.6822 | 3 | 7 |
| 11 | 0.8750 | 0.4771 | 0.6793 | 0.8000 | 0.4888 | 0.6093 | 0.6327 | 6 | 16 |
| 12 | 0.8750 | 0.6312 | 0.8668 | 0.8000 | 0.5755 | 0.7896 | 0.7217 | 2 | 4 |
| 13 | 0.5000 | 0.9543 | 0.5478 | 0.5000 | 0.9162 | 0.5251 | 0.6471 | 4 | 13 |
| 14 | 0.7500 | 1.0000 | 0.7694 | 0.6667 | 1.0000 | 0.6844 | 0.7837 | 1 | 1 |
| 15 | 0.8750 | 0.6818 | 0.4877 | 0.8000 | 0.6111 | 0.4939 | 0.6350 | 5 | 15 |
| 16 | 0.2500 | 0.6191 | 0.4915 | 0.4000 | 0.5676 | 0.4958 | 0.4878 | 9 | 40 |
| 17 | 0.5000 | 0.6708 | 0.3955 | 0.5000 | 0.6030 | 0.4527 | 0.5185 | 8 | 37 |
| 18 | 0.6250 | 0.7712 | 0.4811 | 0.5714 | 0.6860 | 0.4907 | 0.5827 | 7 | 29 |
| 19 | 0.6250 | 0.4116 | 0.5259 | 0.5714 | 0.4594 | 0.5133 | 0.5147 | 9 | 38 |
| 20 | 0.8750 | 0.6164 | 0.6972 | 0.8000 | 0.5659 | 0.6228 | 0.6629 | 3 | 10 |
| 21 | 1.0000 | 0.3920 | 0.7428 | 1.0000 | 0.4513 | 0.6604 | 0.7039 | 2 | 6 |
| 22 | 0.3750 | 0.6949 | 0.5370 | 0.4444 | 0.6210 | 0.5192 | 0.5282 | 8 | 36 |
| 23 | 0.5000 | 0.7904 | 0.3999 | 0.5000 | 0.7046 | 0.4545 | 0.5531 | 7 | 34 |
| 24 | 0.8750 | 0.9526 | 0.6878 | 0.8000 | 0.9133 | 0.6156 | 0.7763 | 1 | 2 |
| 25 | 0.2500 | 0.9528 | 0.6348 | 0.4000 | 0.9137 | 0.5779 | 0.6305 | 4 | 17 |
| 26 | 0.5000 | 0.8269 | 0.5832 | 0.5000 | 0.7428 | 0.5454 | 0.5960 | 6 | 24 |
| 27 | 0.6250 | 0.8743 | 0.5257 | 0.5714 | 0.7991 | 0.5132 | 0.6279 | 5 | 18 |
| 28 | 0.7500 | 0.4929 | 0.9102 | 0.6667 | 0.4965 | 0.8478 | 0.6703 | 2 | 9 |
| 29 | 0.8750 | 0.5093 | 0.4378 | 0.8000 | 0.5047 | 0.4707 | 0.5918 | 5 | 25 |
| 30 | 0.8750 | 0.8495 | 0.1750 | 0.8000 | 0.7687 | 0.3773 | 0.6487 | 3 | 12 |
| 31 | 0.5000 | 0.8373 | 0.2335 | 0.5000 | 0.7545 | 0.3948 | 0.5498 | 9 | 35 |
| 32 | 0.6250 | 0.7169 | 0.3981 | 0.5714 | 0.6385 | 0.4538 | 0.5545 | 8 | 33 |
| 33 | 0.8750 | 0.8440 | 0.3893 | 0.8000 | 0.7622 | 0.4502 | 0.6708 | 1 | 8 |
| 34 | 0.2500 | 0.9073 | 0.5842 | 0.4000 | 0.8437 | 0.5459 | 0.5965 | 4 | 23 |
| 35 | 0.6250 | 0.7660 | 0.3857 | 0.5714 | 0.6812 | 0.4487 | 0.5671 | 7 | 31 |
| 36 | 0.6250 | 0.8242 | 0.4115 | 0.5714 | 0.7398 | 0.4594 | 0.5902 | 6 | 26 |
| 37 | 0.8750 | 0.0000 | 0.8608 | 0.8000 | 0.3333 | 0.7823 | 0.6385 | 3 | 14 |
| 38 | 0.8750 | 0.4416 | 1.0000 | 0.8000 | 0.4724 | 1.0000 | 0.7575 | 1 | 3 |
| 39 | 1.0000 | 0.3809 | 0.5085 | 1.0000 | 0.4468 | 0.5043 | 0.6504 | 2 | 11 |
| 40 | 0.0000 | 0.5547 | 0.0000 | 0.3333 | 0.5289 | 0.3333 | 0.3985 | 9 | 45 |
| 41 | 0.1250 | 0.5641 | 0.0475 | 0.3636 | 0.5342 | 0.3442 | 0.4140 | 7 | 43 |
| 42 | 0.6250 | 0.3880 | 0.0614 | 0.5714 | 0.4496 | 0.3476 | 0.4562 | 6 | 42 |
| 43 | 0.1250 | 0.4928 | 0.0944 | 0.3636 | 0.4964 | 0.3557 | 0.4053 | 8 | 44 |
| 44 | 0.5000 | 0.6275 | 0.3586 | 0.5000 | 0.5731 | 0.4381 | 0.5037 | 4 | 39 |
| 45 | 0.6250 | 0.5021 | 0.1692 | 0.5714 | 0.5010 | 0.3757 | 0.4827 | 5 | 41 |

Table 7. Rank order based on the GRG.

| Level | Filler % | Drill bit diameter | Spindle speed & feed rate |
|-------|---------------|--------------------|---------------------------|
| 1 | 0.6052 | 0.6515 | 0.5658 |
| 2 | 0.6324 | 0.5848 | 0.6005 |
| 3 | 0.6215 | 0.5556 | 0.6257 |
| 4 | 0.6044 | – | – |
| 5 | 0.5230 | – | – |

Table 8. Mean GRG at various levels of drilling parameters.**Fig. 9.** Response graph for the GRG.

Data availability

All data relevant to the study are included in the article. In addition, the datasets used and/or analyzed during the current study are available from the corresponding author on reasonable request.

Received: 4 November 2024; Accepted: 25 February 2025

Published online: 04 March 2025

References

1. He, H. et al. Enhanced distribution and mechanical properties of high content nanoparticles reinforced metal matrix composite prepared by flake dispersion. *Compos. Part B: Eng.* **252**, 110514. <https://doi.org/10.1016/j.compositesb.2023.110514> (2023).
2. El-Sombaty, I., Khashaba, U. A. & Machaly, T. Factors affecting the machinability of GFR/epoxy composites. *Compos. Struct.* **63**, 329–338. [https://doi.org/10.1016/S0263-8223\(03\)00181-8](https://doi.org/10.1016/S0263-8223(03)00181-8) (2004).
3. Natarajan, E. et al. Drilling-induced damages in hybrid carbon and glass fiber-reinforced composite laminate and optimized drilling parameters. *J. Compos. Sci.* **6**(10), 310. <https://doi.org/10.3390/jcs6100321> (2022).
4. Goutham, E. R. et al. Drilling parameters and post-drilling residual tensile properties of natural-fiber-reinforced composites: A review. *J. Compos. Sci.* **7**, 136. <https://doi.org/10.3390/jcs7040136> (2023).
5. Mohan, N. S., Kulkarni, S. M. & Ramachandra, A. Delamination analysis in drilling process of glass fiber reinforced plastic (GFRP) composite materials. *J. Mater. Process. Technol.* **186**, 265–271. <https://doi.org/10.1016/j.jmatprotec.2006.12.043> (2007).
6. Ghasemi, F. A., Hyvadi, A., Payganeh, G. & Arab, N. B. M. Effects of drilling parameters on delamination of glass-epoxy composites. *Aust. J. Basic Appl. Sci.* **5**, 1433–1440 (2011).

7. Antil, P., Singh, S., Manna, A., Katal, N. & Pruncu, C. An improvement in drilling of Sicp/glass fiber-reinforced polymer matrix composites using response surface methodology and multi-objective particle swarm optimization. *Polym. Compos.* **42**, 5051–5064. <https://doi.org/10.1002/pc.26204> (2021).
8. Demircan, Ö. et al. Compression after impact and Charpy impact characterizations of glass fiber/epoxy/mwcnt composites. *Fiber Polym.* **21**, 1824–1831. <https://doi.org/10.1007/s12221-020-9921-9> (2020).
9. Yim, D., Park, J., Jang, S., Choi, J. & Park, N. H. Fabrication and properties of glass fiber-reinforced composites using polyimide Prepregs with inorganic nanofillers. *Fiber Polym.* **22**, 804–810. <https://doi.org/10.1007/s12221-021-0148-1> (2021).
10. Nallusamy, S. Characterization of epoxy composites with TiO₂ additives and E-Glass fibers as reinforcement agent. *J. Nano Res.* **40**, 99–104 (2016). <https://doi.org/10.4028/www.scientific.net/jnanor.40.99>
11. Singh, A. & Jayswal, S. C. Mechanical characterization of TiO₂ nanoparticles based on glass fiber reinforced polymer composite. *IOP Conf. Ser.: Mater. Sci. Eng.* **1206**, 012006. <https://doi.org/10.1088/1757-899x/1206/1/012006> (2021).
12. Abass, B. A., Hunain, M. B. & Khudair, J. M. Effects of titanium dioxide nanoparticles on the mechanical strength of epoxy hybrid composite materials reinforced with unidirectional carbon and glass fibers. *IOP Conf. Ser. Mater. Sci. Eng.* **1094**, 012159. <https://doi.org/10.1088/1757-899x/1094/1/012159> (2021).
13. Tüzemen, M. Ç., Khakzad, F. & Salamci, E. Investigation of tensile properties of glass fiber/epoxy nanocomposites laminates enhanced with graphene nanoparticles. *Fiber Polym.* **22**, 1441–1448. <https://doi.org/10.1007/s12221-021-0521-0> (2021).
14. Megahed, M., Youssef, S. M., Ali-Eldin, S. S. & Agwa, M. A. Upgraded mechanical properties of diluent nano-filled glass/epoxy composites fabricated by vacuum assisted resin infusion. *Fiber Polym.* **22**, 1063–1081. <https://doi.org/10.1007/s12221-021-0210-z> (2021).
15. El-Ghaoui, K., Chatelain, J. F. & Ouellet-Plamondon, C. Effect of graphene on machinability of glass fiber reinforced polymer (GFRP). *J. Manuf. Mater. Process.* **3**, 78. <https://doi.org/10.3390/jmmp3030078> (2019).
16. Kumar, J., Verma, R. K. & Debnath, K. A new approach to control the delamination and thrust force during drilling of polymer nanocomposites reinforced by graphene oxide/carbon fiber. *Comp. Struct.* **253**, 112786. <https://doi.org/10.1016/j.compstruct.2020.112786> (2020).
17. Thakur, R. K. & Singh, K. K. Influence of fillers on polymeric composite during conventional machining processes: A review. *J. Braz Soc. Mech. Sci. Eng.* **43**, 94. <https://doi.org/10.1007/s40430-021-02813-z> (2021).
18. Kharwar, P. K., Verma, R. K. & Singh, A. Neural network modeling and combined compromise solution (CoCoSo) method for optimization of drilling performances in polymer nanocomposites. *J. Thermoplast. Compos. Mater.* **35**(10), 1604–1631. <https://doi.org/10.1177/0892705720939165> (2020).
19. Alvarado, C. C. et al. Melt-mixed thermoplastic nanocomposite containing carbon nanotubes and titanium dioxide for flame retardancy applications. *Polymers* **11**(7), 1204. <https://doi.org/10.3390/polym11071204> (2019).
20. Mirabedini, A. et al. Evolving strategies for producing multiscale graphene-enhanced fiber-reinforced polymer composites for smart structural applications. *Adv. Sci.* **7**, 1903501. <https://doi.org/10.1002/advs.201903501> (2020).
21. Reddy, R. H. N. et al. Evaluating the wear studies and tool characteristics of coated and uncoated HSS drill bit—A review. *Mater. Today Proc.* **46**, 3779–3785. <https://doi.org/10.1016/j.matpr.2021.02.022> (2021).
22. Babu, J., Madarapu, A., Tom, S. & Ramana, M. V. Multi characteristic optimization of high-speed machining of GFRP laminate by hybrid Taguchi desirability approach. *Mater. Today Proc.* **58**, 238–243. <https://doi.org/10.1016/j.matpr.2022.02.097> (2022).
23. Sayin, A. Ç. et al. Experimental and statistical damage analysis in milling of S2-glass fiber/epoxy and basalt fiber/epoxy composite. *Polym. Comp.* **45**(16), 15140–15158. <https://doi.org/10.1002/pc.28826> (2024).
24. da Silva, D. N. R. *Image Processing Methodology for Assessment of Drilling Induced Damage in CFRP* (Universidade Nova de Lisboa, 2013).
25. Gugulaoth, B., Rao, G. K. M. & Bezabih, M. Grey relational analysis for multi-response optimization of process parameters in green electrical discharge machining of Ti-6Al-4V alloy. *Mater. Today Proc.* **46**, 89–98. <https://doi.org/10.1016/j.matpr.2020.06.135> (2021).
26. Julong, D. Introduction to grey system theory. *J. Grey Syst.* **1**, 1–24 (1989).
27. Çelik, Y. H., Kilickap, E. & Koçyiğit, N. Evaluation of drilling performances of nanocomposites reinforced with graphene and graphene oxide. *Int. J. Adv. Manuf. Technol.* **100**, 2371–2385. <https://doi.org/10.1007/s00170-018-2875-z> (2018).
28. Khashaba, U., El-Sonbaty, I., Selmy, A. & Megahed, A. Drilling analysis of woven glass fiber-reinforced/epoxy composites. *J. Compos. Mater.* **47**, 191–205. <https://doi.org/10.1177/0021998312438620> (2012).
29. Kavad, B. V., Pandey, A. B., Tadavi, M. V. & Jakharia, H. C. A review paper on effects of drilling on glass fiber reinforced plastic. *Proc. Technol.* **14**, 457–464. <https://doi.org/10.1016/j.protcy.2014.08.058> (2014).
30. Anand, R. L., Gaitonde, V. N. & Desai, B. Machinability studies of cenosphere reinforced epoxy composites. *Mater. Today Proc.* **5**, 25509–25518. <https://doi.org/10.1016/j.matpr.2018.10.357> (2018).
31. Abrão, A. M., Rubio, J. C. C., Faria, P. E. & Davim, J. P. The effect of cutting tool geometry on thrust force and delamination when drilling glass fibre reinforced plastic composite. *Mater. Des.* **29**, 508–513. <https://doi.org/10.1016/j.matedes.2007.01.016> (2008).
32. Latha, B. & Senthilkumar, V. S. Analysis of thrust force in drilling glass fiber-reinforced plastic composites using fuzzy logic. *Mater. Manuf. Process.* **24**, 509–516. <https://doi.org/10.1080/10426910802714688> (2009).
33. Mohan, N. S., Ramachandra, A. & Kulkarni, S. M. Influence of process parameters on cutting force and torque during drilling of glass-fiber polyester reinforced composites. *Compos. Struct.* **71**, 407–413. <https://doi.org/10.1016/j.compstruct.2005.09.039> (2005).
34. Kilickap, E. Analysis and modeling of delamination factor in drilling glass fiber reinforced plastic using response surface methodology. *J. Compos. Mater.* **45**, 727–736. <https://doi.org/10.1177/0021998310381539> (2010).
35. Ragunath, S., Velmurugan, C. & Kannan, T. Optimization of drilling delamination behavior of GFRP/clay nano-composites using RSM and GRA methods. *Fibers Polym.* **18**, 2400–2409. <https://doi.org/10.1007/s12221-017-7420-4> (2017).
36. Agnihotri, S. N., Thakur, R. K. & Singh, K. K. Influence of nanoclay filler on mechanical properties of CFRP composites. *Mater. Today Proc.* **66**, 1734–1738. <https://doi.org/10.1016/j.matpr.2022.05.270> (2022).
37. Krishnaraj, V. et al. Optimization of machining parameters at high speed drilling of carbon fiber reinforced plastic (CFRP) laminates. *Compos. Part: B* **43**, 1791–1799. <https://doi.org/10.1016/j.compositesb.2012.01.007> (2012).
38. Heidary, H., Karimi, N. Z. & Minak, G. Investigation on delamination and flexural properties in drilling of carbon nanotube/polymer composites. *Compos. Struct.* **201**, 112–120. <https://doi.org/10.1016/j.compstruct.2018.06.041> (2018).

Author contributions

M.S.H., V.S.H.K., M.B.P., N.A., S.M.K.T. conceptualized, curated data, performed formal analysis, visualized, investigated, developed software, and wrote the original draft. C.M. curated data, performed formal analysis, investigated, developed software, visualized, and wrote the original draft. S.K. investigated, developed software. L.F.N. performed methodology and formal analysis and wrote the original draft. N.J. investigated, developed software. All authors reviewed the manuscript.

Declarations

Competing interests

The authors declare no competing interests.

Additional information

Correspondence and requests for materials should be addressed to S.M.K.T. or N.A.

Reprints and permissions information is available at www.nature.com/reprints.

Publisher's note Springer Nature remains neutral with regard to jurisdictional claims in published maps and institutional affiliations.

Open Access This article is licensed under a Creative Commons Attribution-NonCommercial-NoDerivatives 4.0 International License, which permits any non-commercial use, sharing, distribution and reproduction in any medium or format, as long as you give appropriate credit to the original author(s) and the source, provide a link to the Creative Commons licence, and indicate if you modified the licensed material. You do not have permission under this licence to share adapted material derived from this article or parts of it. The images or other third party material in this article are included in the article's Creative Commons licence, unless indicated otherwise in a credit line to the material. If material is not included in the article's Creative Commons licence and your intended use is not permitted by statutory regulation or exceeds the permitted use, you will need to obtain permission directly from the copyright holder. To view a copy of this licence, visit <http://creativecommons.org/licenses/by-nc-nd/4.0/>.

© The Author(s) 2025